A Self-Consistent-Field Analysis of the Surface Structure and Surface Tension of Partially Fluorinated Copolymers: The Influence of Polymer Architecture

R. D. van de Grampel,[†,§] W. Ming,[†] J. Laven,[*,†] R. van der Linde,[†] and F. A. M. Leermakers[‡]

Laboratory of Polymer Chemistry and Coatings Technology, Eindhoven University of Technology, P.O. Box 513, 5600 MB Eindhoven, The Netherlands, and Laboratory of Physical and Colloid Science, Wageningen University, P.O. Box 8038, 6700 EK Wageningen, The Netherlands

Received December 17, 2001; Revised Manuscript Received April 10, 2002

ABSTRACT: A molecular-level self-consistent-field theory is used to analyze physical and thermodynamic properties of partially fluorinated poly(methyl methacrylate) chains in the vicinity of the polymer−vapor interface. The molecules are described on a united atom level in which the methyl ester and perfluoroalkyl esters are linked onto a C−C backbone, whereas the vapor is modeled as free volume. Replacing $-OCH_3$ groups by $-OCH_2C_6F_{13}$ groups was used to vary the chain composition/architecture. In agreement with experimental data, the degree of fluorination influences the surface tension in a nonlinear way; a small fraction of fluorinated groups leads to a relatively large drop of the surface tension. The surface characteristics also depend on various polydispersity effects. The effects of chain length, blockiness, and degree of incorporation of the fluorinated monomer were systematically analyzed. It is found that both the surface tension and surface structure are very sensitive to the degree of blockiness, leading in special cases to microphase separation of the bulk. For these microphase-separated systems a completely ordered bulk with lamellae parallel to the surface was observed.

1. Introduction

Wettability, low adhesion to the surface, and friction resistance of polymeric coatings are material properties that are controlled by the composition of the outermost surface layer. Such coatings may contain several constituents, one or a few of which may adsorb preferentially at the surface. It follows from the classical Gibbs adsorption law that in these multicomponent systems the surface concentration differs from that in the bulk. Typically, the surface is enriched with the component with the lowest surface tension. Surface segregation phenomena have, for example, been observed in polymer blends,[1] solutions,[2] and block copolymers.[3] This surface enrichment can be useful to design an "ideal" coating system that combines the best bulk properties with the optimized surface properties.

The driving force for surface segregation in these systems is related to the lowering of the free energy. When the surface area is fixed, e.g., by the macroscopic dimensions of the system, the excess free energy of the surface per unit area (the surface tension γ) is the only parameter that is left to minimize the free energy of the system.

It is known that the surface tension of a random copolymer melt is, in many cases, almost linearly related to the molar fraction of its monomer units.[4] Recently, surface segregation phenomena have been observed in monocomponent polymer systems containing pendent perfluoroalkyl side groups, comparable to what was found with polymer blends. In such cases only part of the polymers, viz. the fluorinated side groups, are preferentially adsorbed in the coating−air interface.[5−10] These surface anisotropic conformations lead to a relatively low free energy density at the surface when incorporating only small amounts of fluorinated moieties. This has been confirmed by X-ray photoelectron spectroscopy (XPS),[11] secondary ion mass spectroscopy (SIMS),[12] forward recoil spectroscopy (FRES),[13] near-edge X-ray absorption fine structure (NEXAFS),[14] and the highly surface sensitive low-energy ion scattering (LEIS).[15] The quantitative analysis of the surface structure, however, is still a matter of extensive research.[16]

Considering the technical difficulties associated with surface analysis (such as high vacuum, possible surface damage during measurement, and unambiguous calibration of the signal), it is of interest to complement chemical−physical measurements by appropriate theoretical modeling. In this paper a detailed self-consistent-field (SCF) theory will be used for this purpose. Self-consistent-field (SCF) theories are known to be applicable to dense polymeric systems because the excluded-volume correlations are screened to a large extent.

Although polymer blend systems are studied extensively, relatively little work on "neat" copolymer systems has been published. In this paper a detailed study of surface segregation effects in a well-defined system of copolymers is presented. The SCF method enables surface composition and surface tension to be determined. Additionally, the effects of chain length, chemical variations, and molecular architecture on surface composition and surface tension are considered. All these aspects can be included in a detailed molecular model in which the size and the shape of the molecule up to the level of monomer units are accurately accounted for.

The remainder of this paper is organized as follows. First, a short introduction to molecular modeling of polymer systems will be given, followed by a review of the basic concepts of the SCF technique. In this review

[†] Eindhoven University of Technology.
[‡] Wageningen University.
[§] Current address: GE Plastics, Bergen op Zoom, The Netherlands.

10.1021/ma0121870 CCC: $22.00
Published on Web 06/04/2002

a more compact formalism is given for branched polymers[17] within the SCF method of Scheutjens and Fleer.[18,19] Additionally, the molecules and the parameters used in the model are described. Subsequently, the results of the SCF analyses will be presented and compared to available experimental data. Conclusions are summarized in the last section.

2. Molecular Modeling

Molecular modeling of the surface properties of polymer materials may be used to help to understand the regularities found in these systems, viz. to obtain detailed conformational results on an atomic level. In molecular dynamics simulations one uses essentially Newton's law, $F = ma$, to trace the molecules and atoms in space and time. There are commercially available software packages in which molecules can be defined in full molecular detail, including the hydrogen atoms. Typically this approach can be used to answer questions about materials, related to the nanometer length scale and nanosecond time scale domains. Changes in chain conformations, surface reorganizations, and the exchange of surface active molecules with less surface active molecules take place on much larger time scale, thus for such purpose an all-atom MD technique cannot be used due to computational limitations. One option is *to coarse grain* the simulations and probe on a larger length and time scale. One of the problems is to find appropriate interaction parameters and the corresponding time scales in these reduced approaches. If dynamical information is only used to investigate the degree of equilibration, one can also use the Monte Carlo (MC) technique to sample the conformational properties in the system. This technique becomes very efficient if molecules are placed on a lattice, such as in the bond fluctuation model (BFM). The BFM technique has been used frequently to study polymer blends and polymer surfaces.[20]

In simulations one can, in principle, account for all possible excluded-volume correlations. The positions of all segments in the system are known at any moment. However, the struggle with the statistical accuracy is always there, and especially for large systems wherein the polymer chains are densely packed, the equilibration is very time demanding. Moreover, it is very difficult to "measure" the appropriate thermodynamic parameters, such as the surface tension, in a simulation.

Thermodynamic properties are readily available if the partition function of the system is known. The only types of partition functions that can be solved are those in which mean-field approximations are used. In polymer physics the mean-field approach is based upon the Edwards diffusion equation:[21]

$$\frac{\partial G(r,N)}{\partial N} = \frac{1}{6}\nabla^2 G(r,N) - u(r)\, G(r,N) \qquad (1)$$

where $G(r,N)$ denotes the probability distribution of finding the end segment N of a polymer chain at coordinate r.

This equation features the behavior of a test chain in an average self-consistent potential field $u(r)$. This potential field is a function of the local density of the various segments. The exact analytical solution of the Edwards equation is known only for very few systems. Typically these equations have to be solved numerically. A discretization scheme, as first suggested by Scheutjens and Fleer[18,19] in the context of polymer adsorption, is utilized in this paper. This approach has successfully been used in a wide range of interfacial systems, e.g. polymer surfactant adsorption, solid/liquid interfaces, polymeric melts, polymeric solutions, self-assembly of copolymers and surfactants, and polymeric brushes.[22] Recently, also transitions between adsorbed chains and so-called flowers have been analyzed.[23] Leermakers[24] used the approach to model the self-assembly of lipid molecules in bilayer membranes. The lipid molecules consist of branched chains in which the united atoms concept, i.e. segments such as CH_2 and CH_3, is used. Polar, apolar, and even charged entities can be descibed. This model will be applied in this paper to deal with the partially fluorinated copolymer systems.

In a SCF, the calculations are coarse-grained such that the degree of freedom on the monomer length scale are ignored. Indeed, the classical approach is to replace one or more monomeric building blocks by one statistical segment.[25] Such an approach is of interest to investigate universal effects in these systems and will be used below when the dependence of the interfacial free energy on the degree of polymerization of the polymer chains will be discussed. However, when the main interest is in the structure of the interfacial layer on the (sub)monomeric length scale, it is important to include the structural characteristics on the segment scale. In this paper the detailed structure of the polymer chains will be included. The conformational characteristics of interfacial molecules on the subsegment level will be predicted.

3. Theory

A. Discretization Scheme for Branched Systems within the Scheutjens−Fleer Theory. The Edwards equation (1) needs to be generalized to account for (i) the presence of more than one segment type along the chain, i.e., not all segments feel the same self-consistent potential, and (ii) the nontrivial chain connectivity (branched chain architecture). Both generalizations are possible and documented in the literature.[17,26] However, a short review of these extensions is of use. We will introduce a compact formalism which is suitable both for linear and for branched chains.

Within the framework of the Scheutjens−Fleer model, the continuous differential equation (1) transforms into a discrete propagator formalism. Within this formalism, it is important that the segments of molecule i have fixed segment ranking number, $s = 1, 2, ..., N$. Subsequently, it is necessary to know the segment type of each segment. A composition operator $\delta^x_{i,s}$ is introduced, which assumes the value unity when segment s of molecule i is of type x and zero otherwise. This operator will be used to select the appropriate weighting factor in the propagators defined below.

The start is to define the Boltzmann weight that accounts for the self-consistent field felt by segment s of molecule i; we write

$$G_i(z,s) = \sum_x G_x(z)\delta^x_{i,s} \qquad (2)$$

where the segment type dependent Boltzmann weights are given by

$$G_x(z) = \exp[-u_x(z)] = \exp\{-[u'(z) + \sum_y \chi_{xy}(\langle\varphi_y(z)\rangle - \varphi^\beta_y)]\} \qquad (3)$$

This equation defines the dimensionless (scaled by kT) self-consistent segment potential $u_x(z)$ felt by a segment of type x at coordinate z along the z-axis. This potential is normalized with respect to a reference phase indicated by the superindex β. By way of normalization, the weighting factors $G_x(z)$ are defined to be unity in this reference phase. Here the vapor phase will be used, which is (extremely) dilute in polymer, as the reference. Alternatively, it would be possible to choose a homogeneous polymer-rich phase as the reference phase. This choice is problematic as soon as the polymer system becomes structured on the microscopic length scales. Apart from these obvious problems, there is no important consequence for the choice of the reference system.

As can be seen in the square brackets of eq 3, the segment potential contains two terms. The first quantity on the right-hand side of eq 3, $u'(z)$, is a Lagrange field (a hard core potential) coupled to the constraint $\sum_x \varphi_x(z) = 1$ in each layer. Here the volume fractions that refer to a particular segment type are computed from corresponding molecule type and ranking number dependent quantities:

$$\varphi_x(z) = \sum_i \sum_{s=1}^{N_i} \varphi_i(z,s)\delta_{i,s}^x \tag{4}$$

These ranking number dependent volume fractions are calculated with the propagator formalism.

The second term in the segment potential eq 3, $\sum_y \chi_{xy}(\langle\varphi_y(z)\rangle - \varphi_y^\beta)$, accounts for the nearest-neighbor contact interactions felt by segment of type x in layer z. It is a summation over all segment types y, including the free volume component, i.e., with $y = V$ (vacuum). In this contribution the Flory−Huggins interaction parameters, χ_{xy}, occur. Below these parameters will be discussed in more detail. The angular brackets in eq 3 denote a three-layer average of the segment density:

$$\langle\varphi(z)\rangle = \frac{\varphi(z-1) + \varphi(z) + \varphi(z+1)}{3} \tag{5}$$

The composition of the reference phase is fully specified by the volume fractions of all the components $\varphi_x^\beta = \sum_i \sum_s (\varphi_i^\beta/N_i)\delta_{i,s}^x$. In principle, it is thus possible to compute the segment potentials from the segment volume fraction profiles. In the SCF approach the reversed action (calculating the volume fractions from the potentials) is also defined.

To compute the segment density profiles from the potentials, it is necessary to first specify uniquely how the segments in the chain are connected to each other. The number of segment−segment bonds is always one less than the number of segments. Let us denote them with bond ranking numbers $t = 1, ..., N - 1$. It is necessary to know the segment ranking numbers that are on both sides of a given bond. These two segments can be specified by sub- and superindices: $t_{s_1}^{s_2} = t_{s_2}^{s_1}$. A segment can be involved in one (chain end), two (middle segment), three, or four (branched segment) bonds. Let t_s be the set of bonds connected to segment s.

In the following we will first introduce the appropriate Greens function G, which is the quantity that collects the overall statistical weight of all possible and allowed conformations of particular chain fragments. This quantity is rather complicated in this case because the chains are branched. Then, a discussion will be given how one can compute these functions starting from the chain ends and propagating along the chain. Finally, it is shown how these functions can be used to obtain the observable segment density profiles.

The Greens function, which may be referred to as the end-point distribution function, is defined as $G_i(z,s,t_s^{s'})$. It reflects the statistical weight of that part of the polymer molecule in which s is the "end-point" segment; the bond $s-s'$ is not yet connected. In other words, this quantity contains the combined statistical weights of (complete, i.e., propagated from chain ends) chain fragments that contain segment s at coordinate z with the extra requirement that fragments are not connected to segment s from the side of bond $t_s^{s'}$. This means that this bond $t_s^{s'}$ is available for the next propagator step. A branched polymer has more than two chain ends. Each chain end has only one bond. Such a chain end can also operate as an "end point". If the walk is started at such an end point, the starting condition is

$$G_i(z,s,t_s^{s'}) = G_i(z,s) \tag{6}$$

where s' is again the segment following to the end segment s, where the walk is started.

Having defined the end-point distribution on a chain end, the segment adjacent to the chain end will be considered as the end point s. The corresponding end-point distribution function will be defined. In this case the propagator step in the direction of the free bond can now be expressed by

$$G_i(z,s,t_s^{s'}) = G_i(z,s)\prod_{t_s \neq t_s^{s'}} \langle G_i(z,s'',t_{s''}^{s})\rangle \tag{7}$$

Here the angular brackets indicate a three-layer average as before. The multiple product goes over all bonds in which segment s is involved except the one between s' and s. Actually, eq 7 is a general expression that is applicable to all segments for propagating along a linear chain but also for propagating along a chain with branch points. Note that eq 7 reduces to eq 6 when it is applied to propagate, starting from the end point s. In this case the set of bonds $t_s \neq t_s^{s'}$ is empty.

The segment densities of a particular segment along the chain is found by a generalized composition law:

$$\varphi_i(z,s) = C_i G_i(z,s)\prod_{t_s} \langle G_i(z,s',t_s^{s'})\rangle \tag{8}$$

This equation computes the segment densities for all segments in the chain, i.e., for chain ends (which have only one bond), middle segments (which have two bonds), and branches.

The normalization constant C_i is chosen such that the integral over the density profile is equal to the known number of molecules in the system. Once this constant is known, it is possible to compute the volume fraction of the polymer in the reference system, $C_i = \varphi_i^\beta/N_i$. The distribution of free volume is found by

$$\varphi_V(z) = (1 - \sum_{i \neq V} \varphi_i^\beta) G_V(z) \tag{9}$$

The above set of equations is closed and is routinely solved by a computer. In the solution, the segment densities both *determine* the segment potentials and *follow from* the segment potentials. In addition, the space-filling constraint (volume fractions including the free volume add up to unity) is obeyed in each coordi-

nate. Typically, the density profiles are obtained with seven or more significant digits. From the self-consistent solution, it is possible to compute all thermodynamic properties, including for example the interfacial tension.

B. Evaluation of the Surface Tension. The evaluation of the surface tension is intrinsically difficult, because it involves the difference between two large contributions, i.e., the difference between the overall free energy and that of the bulk. Only those contributions that are in excess of the bulk have to be accounted for. However, in the SCF theory the evaluation of the grand potential per unit area, i.e., the dimensionless surface tension $\tilde{\gamma}$, is evaluated straightforwardly from the segment density and the potential profile:

$$\tilde{\gamma} = -\sum_{z=1}^{M}\left[\sum_{i}\frac{\varphi_i(z)-\varphi_i^{\beta}}{N_i} + \sum_{A} u_A(z)\,\varphi_A(z) - \frac{1}{2}\sum_{A,B}\chi_{AB}[\varphi_A(z)\langle\varphi_B(z)-\varphi_B^{\beta}\rangle - \varphi_A^{\beta}(\varphi_B(z)-\varphi_B^{\beta})]\right] \quad (10)$$

1. Surface Tension of a Molecularly Homogeneous Bulk in Equilibrium with a Vapor. It should be clear from the above that the SCF calculations are done on closed systems, in systems wherein the temperature T, the volume V, and the number of molecules n are fixed. In this system the conformations and density profiles are adjusted such that the Helmholtz energy is minimal.

Calculations are typically done on a discrete set of coordinates (a lattice). It is common that gradients in densities develop that are not negligible on the discretization length scale (strong segregation limit). Then so-called lattice artifacts may occur. These problems are best shown when the interface is shifted with respect to the discretization points (lattice). Typically we will observe that the chemical potentials as well as the surface tension become functions of the position of the interface. One way to view these artifacts is that there exists some stress in the system as long as the interface is not placed optimally with respect to the grid. This stress can be viewed upon as a type of lattice pressure Δp. Then the chemical potentials of the molecules are given by

$$\mu_i = \mu_i^{\mathrm{FH}} + N_i\Delta p \quad (11)$$

where μ^{FH} is the chemical potential as given by the Flory−Huggins theory, corresponding to the binodal value. The Gibbs−Duhem relation for interfacial systems reads

$$\partial\gamma = -\sum_{i} n_i\partial\mu_i \quad (12)$$

from which it is seen that the surface tension in the system is a function of the position of the interface as well. Only when the lattice pressure vanishes, i.e., when $\mu = \mu_i^{\mathrm{FH}}$ (binodal), is the Helmholtz energy minimal. This provides a straightforward way to compute the optimal position of the interface and therefore the unperturbed surface tension.

There exists an alternative method to find a good estimate of the artifact-free surface tension. In this method the interface is shifted in small steps over a distance of one lattice site. As a result, a quasi-sinusoidal variation of the interfacial tension is obtained. The artifact-free point is found when the average of these interfacial tensions is computed, i.e., halfway the period of the oscillation. This method is used in this paper.

2. Surface Tension for a System Wherein the Bulk Is Microphase Segregated. Next the case will be considered that the bulk is no longer completely homogeneous in density. Indeed, it is possible that the bulk has some structure on the molecular scale. This is called microphase separation. The calculation of the interfacial tension of the system in which the polymer phase is microphase separated cannot proceed along the same lines as specified in case (1). The reason for this is that the Flory−Huggins theory does not give direct access to the chemical potentials that should be used to find the point with a vanishing lattice pressure. For this reason it proves necessary to perform separate calculations to investigate the equilibrium properties of the microphase-separated bulk phase.

It must be true that a macroscopic amount of the microphase segregated system has no interfacial tension associated with the presence of the local density variations. In the calculations, it is not possible to impose this constraint directly onto the calculations. However, it is possible to investigate the "unit cell" properties of the system in the SCF approach systematically. In such a particular calculation it is necessary to preassume the volume of the small system under investigation; i.e., it is necessary to fix the length of the unit cell. Let us refer to this length by the variable M. Reflecting boundary conditions on both sides of the small system implies that the unit cell is copied on either side of the system boundaries. The amount of polymer, and thus the amount of free volume, is varied until the grand potential of the system vanishes. (Again, eq 10 may be used to find the interfacial tension in the small system.) Of course, it is necessary to vary the system size M and repeat the calculations. Of interest is the Helmholtz energy density, i.e., $f(M) = F(M)/(M)$. The optimal unit cell length M^* corresponds to the minimum of $f(M)$. The chemical potential of the polymers that occurs at the optimal unit cell size, μ^*, is of course available from such analysis.

From this point on, it is possible to follow the procedure discussed above to obtain the surface tension of the polymer−vapor interface. Now the chemical potential of the optimized bulk μ^* takes the role of the μ^{FH} (binodal). The optimal position of the interface, i.e., for which the polymer bulk is fully relaxed (where there is no lattice pressure), occurs when the chemical potential of the polymers equals μ^*. The grand potential per unit area of this system corresponds to the requested artifact-free surface tension.

C. The Molecules. The structure of a particular polymer chain is defined by the sequence of MMA and F6MA units. The following notation will be used. A regular or block copolymer will be represented by *r* or *b*, respectively. Thus, *r*-$(MMA)_{55}(F6MA)_5$ is a regular copolymer of 55 units of MMA and 5 units of F6MA, whereas *b*-$(F6MA)_5(MMA)_{55}$ is a block structure. Typically, the sequence of monomer units in the regular copolymer *r*-$(MMA)_{55}(F6MA)_5$ is that each unit of F6MA is followed by 11 MMA units. In another example, *r*-$(MMA)_{50}(F6MA)_{10}$, every unit of F6MA is followed by 5 units of MMA. Furthermore, *r*-$(MMA)_{30}(F6MA)_{30}$ is an alternating copolymer of units of MMA and F6MA.

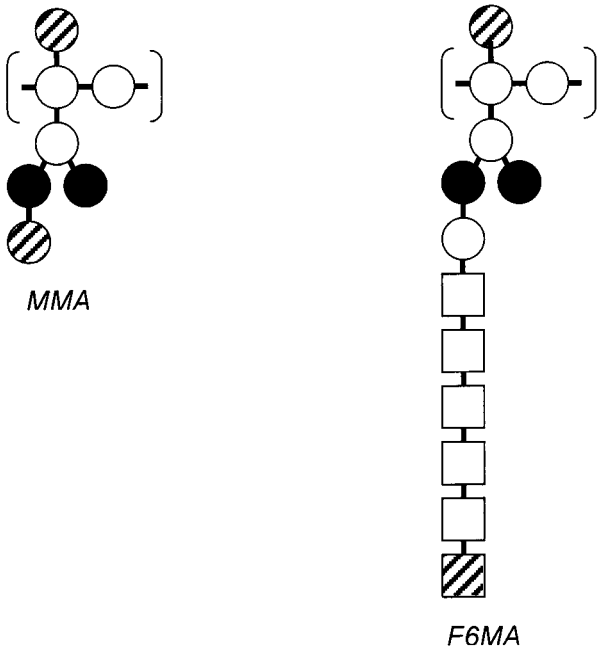

Figure 1. A representation of the building blocks of the molecules used in this study. On the left the methyl methacrylate monomer unit (MMA) and on the right 1,1-dihydroperfluoroheptyl methacrylate (F6MA) are depicted. The open circles represent the CH_x groups (x = 0, 1, or 2), the black circles are oxygens, the striped circle is the CH_3 group, the open squares is a CF_2, and the striped square is the CF_3 group.

The number of units of MMA between two units of F6MA is represented by m.

Note the difference between b-$(MMA)_{27}(F6MA)_5$-$(MMA)_{28}$ and b-$(MMA)_{55}(F6MA)_5$. They have the same overall composition, but the sequence of five F6MA units is in the first case positioned in the center of the molecule, whereas in the latter the F6MA units are at one of the chain ends.

To get a realistic description of the system, it is important to accurately account for the size and shape of molecules, i.e., for the chain architecture. Moreover, information is required about parameters that specify how the various parts of the molecule interact. Here it is important to mention that a lattice gas model is applied in which the system with volume $M*L$ is incompletely filled with polymer units. The unoccupied lattice sites are denoted by the letter V (vacancies/free volume). These two aspects will be discussed in somewhat more detail because of their importance later on.

The molecules are considered to be fully flexible and are allowed to return to previously occupied sites according to the discretized Edward's equation using a first-order Markov approximation. A united atom description is used to represent the molecules (Figure 1). As mentioned previously, the lattice sites can be filled by either x = V, CH_2, CH_3, O, CF_2, CF_3. For all solutions of the SCF equations the volume fractions obey the constraint $\sum_x \varphi_x(z) = 1$ for each layer z. This means that the polymers cannot visit the same sites too often, because otherwise the density of the polymers will exceed unity.

D. The Parameters. The interactions in the system are parametrized by the well-known Flory−Huggins (FH) parameters χ_{xy}. Here we face the same problem as in coarse-grained MD simulations: there is no readily set available. As the CPU time needed for SCF calculations is orders of magnitude less than MD simulations, one can effort test calculations to find an appropriate set. The values of the parameters must be chosen in such a way that they represent the system as accurately as possible. Because there are 6 different "units", there are 6*5/2 = 15 different segment pairs, the χ's should be found from comparison with experiments. However, the ideal situation that all parameters are known accurately is not yet reached, and "educated guesses" for the Flory−Huggins interaction parameters have to be made. In this respect it is important to realize that the parameters should be consistent with the level of detail that is chosen for the description of the structure of the monomeric building blocks. From the fitting of the phase behavior of the alkane−vapor system, Schlangen[27] recommends $\chi_{V,CH_2} = 1.6$. Unless otherwise specified, the same value has been taken for χ_{V,CH_2}. This point is used as a reference for the other FH values for interaction with unoccupied sites. For example, because the oxygen is more polarizable, it will have a higher FH value and therefore a value of $\chi_{V,O} = 2$ was taken. The effect will be that the hydrocarbon units prefer the polymer−vapor interface to the oxygen atoms. The fluorinated groups on the other hand are poorly polarizable and therefore have a relatively low χ value. Again, fitting appropriate phase diagrams will result in better guesses for these units. Here a value of $\chi_{V,CF_3} = \chi_{V,CF_2} = 1.2$ was taken. Although not optimal, this choice seems reasonable and will reflect the trends of the system qualitatively correct. Fine-tuning the parameter set is possible, but this is not attempted in this work.[28]

Table 1. Short-Range Interaction Parameters

χ	V	CH_x	O	CF_2/CF_3
V	0	1.6	2	1.2
CH_x	1.6	0	1	0.5
O	2	1	0	2
CF_2/CF_3	1.2	0.5	2	0

All SCF calculations were performed, if not otherwise mentioned, for polymer chains consisting of sixty "monomer" units (remember that each monomer is composed out of several united atoms). The short-range interactions, expressed by the Flory−Huggins interaction parameters, are listed in Table 1.

4. Results

As outlined in the Introduction, the macroscopic relationship between the surface tension and properties such as wetting and adhesion is well established. However, the correlation with the microscopic molecular structure of the surface is less well documented. Nevertheless, it is generally accepted that the surface tension is predominantly determined by the compositions in the first atomic layer of the film.[29] Our SCF analyses involve no a priori assumptions about the molecular properties of the surface and near surface layers. Therefore, it is very interesting to compare the outcome of the theoretical analysis with experimental surface data, like contact angle data and angle dependent XPS, conducted on these systems. These and related aspects will be considered in the following sections.

First the surface tensions of regular copolymers of MMA and F6MA, as obtained by our SCF model, will be considered.

A. Surface Tensions. In this section the polymer−vapor interface for regular copolymers of MMA and F6MA is discussed. The interfacial tension ($\tilde{\gamma}$) of a polymer−vapor interface is one of the key properties and

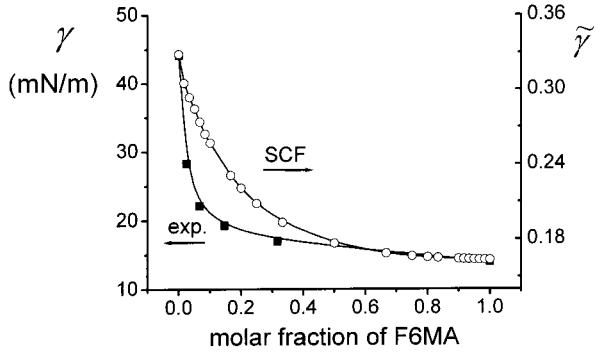

Figure 2. Surface tensions for regular MMA/F6MA copolymers for different molar fractions of F6MA. Calculated SCF results (open points) are compared to experimental data for random copolymers[15] (solid points). The lines are a guide for the eyes.

results from the density and potential profiles of the segments according to eq 10. To investigate the liquid−vapor interface within the SCF theory, the amount of molecules in the system is chosen such that the two phases coexist. The densities of these coexisting phases follow directly the Flory−Huggins theory. As explained above in the SCF calculations of the surface tension, lattice artifacts are eliminated by adjusting the number of molecules (for shifting the position of the interface) until the volume fractions of the coexisting bulk phases equals those calculated with the Flory−Huggins theory. Within this theory the surface tension of the lattice fluid is dimensionless. To convert this value to units of N/m, it has to be divided by the area of a lattice site and multiplied by k_BT:

$$\tilde{\gamma} = \frac{\gamma b^2}{k_B T} \tag{13}$$

where $\tilde{\gamma}$ is the dimensionless surface tension, T the absolute temperature, k_B Boltzmann's constant, and b the lattice parameter of the cubic lattice.

In Figure 2 the calculated surface tension is given as a function of the molar fraction of F6MA. It can be seen that a small increase of the F6MA content in the copolymer results in a significant reduction of the surface tension of the random copolymer. This is consistent with the results obtained experimentally for these systems using contact angle data[15] (also shown in Figure 2).

However, the surface tension as a function of molar fraction of F6MA for the experimental data on random copolymers shows more curvature than for the SCF analyses of regular copolymers, in particular for regions with low content of F6MA. This cannot be explained by the short-range FH interactions between the different segments in the molecules; e.g., changing the χ_{V,CF_3} value from 1.2 to 1 did not affect this difference. From polymer blend studies it is well-known that several other factors influence the polymer−polymer phase and interface behavior as well. Examples are the nature of the monomers, the molecular architecture, composition, and the molecular size of the polymers.[30] The influence of all these factors on the SCF results will be studied systematically, and the results will be discussed in more detail later on in this paper. The next section we will deal first with the general features of the surface structures of these regular copolymers before discussing these points.

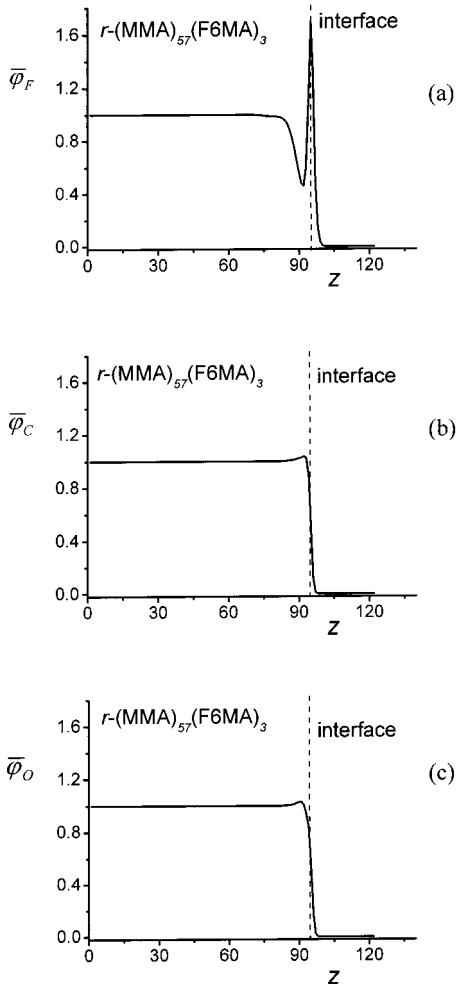

Figure 3. Scaled segment density profiles of (a) $CF_2 + CF_3$ ($\bar{\varphi}_F$), (b) $CH_2 + CH_3$ ($\bar{\varphi}_C$), and (c) O segments ($\bar{\varphi}_O$) in the liquid−vapor interface film of polymer r-$(MMA)_{57}(F6MA)_3$.

B. The Structure of the Surface. One of the main interests of surfaces is the microscopic molecular structure of regular polymers in the polymer−air interface. From a given SCF solution, not only thermodynamic information (surface free energy) is readily obtained, it is also possible to evaluate structural information, i.e., density profiles of the different segments. Generally, the surface tensions of polymer melts are largely determined by the bulk behavior of the fluid. However, surface conformations of functional groups (such as fluorinated tails orient themselves in arrays) maybe pivotal to the minimization of the surface tension. Therefore, the conformation of the polymer chain near the interface was studied in detail. Some typical density profiles for r-$(MMA)_{57}(F6MA)_3$ are given in Figure 3. Figure 3a shows the segmental density of $CF_2 + CF_3$ ($\bar{\varphi}_F$) as scaled with φ_F in the bulk of the polymer phase. In the liquid−vapor interface enrichment in the density of fluorine is observed, pointing to a preferential presence of the perfluorinated alkyl side chains at the boundary of the interface. A depletion zone, as a natural consequence, follows this fluorine-enriched layer. Angle-dependent XPS measurements on these systems did not reveal this depletion layer (see ref 15), probably because of the limited depth sensitivity in these measurements. The minimum of depth resolution is 5 nm for by angle-dependent XPS measurements. Moreover, the intensity of an XPS signal falls off exponentially with the depth.[15]

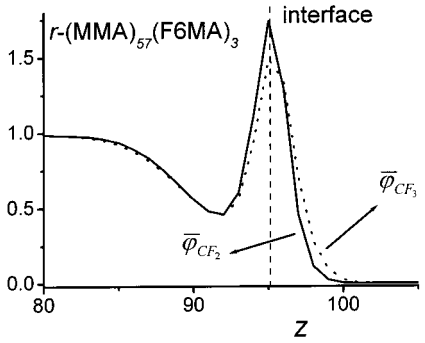

Figure 4. Scaled volume fraction of the CF_2 ($\bar{\varphi}_{CF_2}$) and the CF_3 ($\bar{\varphi}_{CF_3}$) segments at the liquid−vapor interface for polymer r-$(MMA)_{57}(F6MA)_3$.

From the density profiles of fluorine it is clear that the enriched top layer is very thin, typically 1−2 nm. This thin layer is an adsorption layer rather than a stratified layer of phase separated bulk material. Such thin layers have been observed for systems by others using neutron reflection experiments.[10]

The scaled segmental density profiles for carbon ($\bar{\varphi}_C$) and oxygen ($\bar{\varphi}_O$) at the boundary of the coexisting phases (Figure 3, b and c, respectively) show features that differ from that of $\bar{\varphi}_F$. Both atoms are repelled from the surface, and a relatively small maximum is found at the location where φ_F shows a depletion zone.

Finally, the location of the scaled segmental density of the CF_2 and CF_3 at the boundary of the coexisting liquid−vapor phases was considered. Figure 4 reveals that the chain ends of the fluorinated side chains have the highest preference for the "contact zone" with the vapor; i.e., in the vicinity of the surface the CF_3 moieties are preferred over the CF_2 segments. This is in agreement with melt surface tension studies of poly(hexafluoropropene oxide) and Cahn−Hilliard density gradient studies, suggesting that the CF_3 side groups are oriented to the surface.[31] In SCF calculations for the liquid−vapor boundaries of n-alkanes this chain end effect has also been observed and can be explained as follows. First, when chain ends are exposed to the vapor boundary side of the interface, the number of unfavorable segment-vacancy contacts is smaller. Second, the conformation entropy of a chain molecule in the interfacial region is larger when a chain end is pushed out of the interface instead of a string of segments. For our system the origin of the difference is only due to conformation entropy, because both the CF_2 and CF_3 segments were given the same FH interaction parameter.

From Figure 3a it can be seen that there is enrichment in fluorine at the boundary of the coexisting liquid−vapor phases. Depending on the molar concentration of F6MA in the regular copolymer, a secondary and sometimes also a third maximum or higher order maximum is observed. The distance between the first and the second maximum is defined as the depletion thickness:

$$d = z_1 - z_2 \tag{14}$$

where z_1 and z_2 refer to the position of the primary and secondary maximum, respectively. This depletion thickness is decreasing with increasing number of units of F6MA in the copolymer. This effect can be seen in Figure 5 where the scaled segment density of CF_3 plus

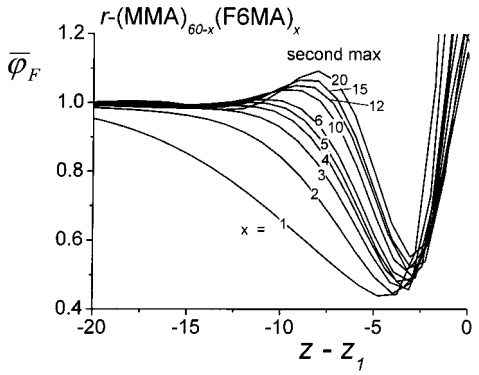

Figure 5. Scaled segmental density profiles of $\bar{\varphi}_F$ fluorine in the subsurface region for r-$(MMA)_{60-x}(F6MA)_x$ with $x = 1$, 2, 3, 4, 5, 6, 10, 12, 15, and 20. The position of the primary maximum is defined as z_1.

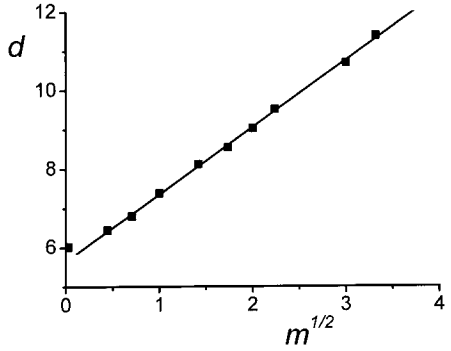

Figure 6. Depletion layer thickness as a function of the square root of the length of the MMA block between two F6MA units in the r-$(MMA)_{60-x}(F6MA)_x$ molecules.

CF_2 moieties near the surface are plotted as a function of $z - z_1$.

Within a chain of r-$(MMA)_{60-x}(F6MA)_x$ the ratio of the number of units of MMA over F6MA (m) is a function of x according to $m + 1 = 60/x$. When m is larger than unity, the physical interpretation of m is the number of MMA units between two F6MA units along the chain. It is interesting that the depletion layer thickness appears to be proportionally to the square root of m in the case of r-$(MMA)_{60-x}(F6MA)_x$ molecules (Figure 6). The depletion zone will be enriched with the MMA units particularly for values of $m > 1$. Gaussian statistics implies that the length scale associated with MMA fragment of length m is given by the square root of m. This length scale dictates the depletion layer thickness. Structurally, this region is expected to be composed of loops and bridges of length m. The loops are chain fragments that return to the same fluorine region from which they depart, and bridges are chain fragment that cross over from one fluorine-rich region to the other. The relative importance of loops vs bridges is presently not clear. Further inspection of Figure 6 reveals that the depletion layer thickness is proportionally to the square root of m even in the region where m is smaller than unity. The loops and bridges picture cannot explain this. In this regime, the surface enrichment indicates that the backbone of the molecules at the surface is predominantly laying parallel to the surface. This alignment is expected to improve for smaller values of m. Fluctuations in the backbone positions increase the depletion layer thickness. Hence, it is not unreasonable to have a square root dependence in the range of $m \leq 1$. Extrapolation to $m = 0$ gives a depletion layer thickness

of approximately 6 lattice units. The dimensions of the perfluoroalkyl side chains must determine this separation. As the length of the side chains is comparable to this limiting depletion layer thickness, it is concluded that the fluorinated side chains are strongly stretched (brush).

C. Chain Length Dependence. As shown in Figure 2, the experimental surface tension decreases much steeper with the addition of small amounts of F6MA than that predicted by the SCF simulations. Therefore, it is interesting to analyze the effect of molar mass on the surface tension and to compare these results with experimental data.

The LeGrand−Gaines relation describes the molecular weight dependency of a homologous series of polymers on the surface tension:[32]

$$\gamma = \gamma_\infty - C_1 M_n^{-x} \tag{15}$$

where M_n denotes the number-average molecular mass, γ_∞ is the surface tension at infinitive molar mass, and C_1 is a semiempirical parameter. The exponent x varies from $^2/_3$ for low molecular weight species to 1 for high molecular weight polymers.

Experimentally, this empirical relation has been found to be valid for *n*-alkanes, perfluoroalkanes, polysiloxanes, and polystyrenes. However, the theoretical interpretation of these results is still a matter of considerable discussion. Poser and Sanches,[33] who follow the Cahn−Hilliard theory,[34] have suggested that the primary contribution arises from the variation of the density of a polymer system with molecular weight. De Gennes[35] and Theodorou[36] suggested that chain conformation entropy causes lower molecular weight components to be preferentially at the surface. Recently, Kumar and Jones[37] found, using mean-field treatments, that density effects are dominating, except in special cases where chain ends are strongly attracted or repelled from the surface. This is in line with the results of Koberstein and co-workers for end-functionalized poly(dimethylsiloxane)s.[38]

To show that the SCF theory applied in this study can be used to evaluate the surface tension of the melt as a function of the molecular weight, first a simplified system was considered. This system is defined as a homopolymer composed of spherical segments of A in a monomeric solvent S with only one FH parameter, viz. $\chi_{A,S} = 1$. This approach enables us to deal with large values of the molecular weights in a straightforward way. Extrapolation to infinite molar mass leads to a value of $\tilde{\gamma}_\infty = 0.01375$. In Figure 7a $\log(\tilde{\gamma}_\infty - \tilde{\gamma})$ is plotted as a function of $\log(M)$. In accordance with the LeGrand−Gaines relation, we find a slope of −1 for high molar mass. Going to lower molecular weight, a gradual deviation of this slope to a lower value is observed, reaching finally a value in the order of −2/3. It should be mentioned that this value is not found over a sufficiently large range of molecular mass and therefore cannot be considered as a scaling law result, especially because $\tilde{\gamma}$ at these low molar masses vanishes due to the appearance of a critical point.

A similar analysis has been carried out for the MMA−F6MA copolymer system. In this case it is necessary to increase the molecular weight at a fixed overall MMA−F6MA composition to exclude composition fluctuation effects. As repeating unit, $(MMA)_2(F6MA)_1(MMA)_2$ block was chosen. Because of the molecular details in this

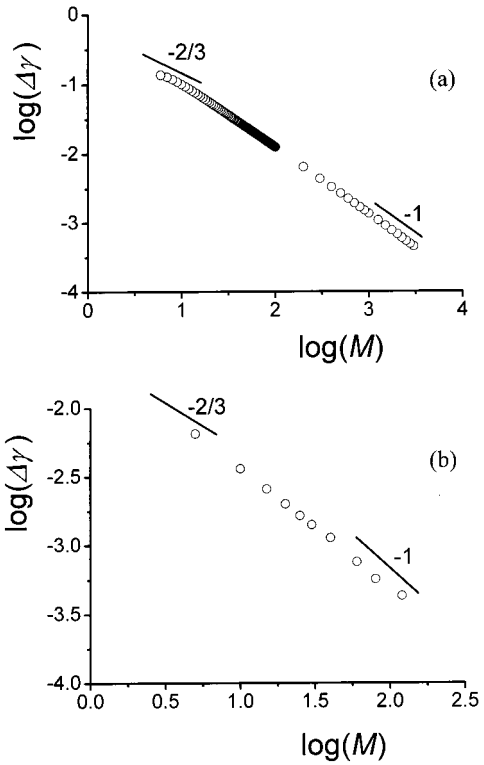

Figure 7. Surface tension dependency on the chain length. Plotted is $\log(\Delta\gamma) = \log(\tilde{\gamma}_\infty - \tilde{\gamma})$. At high M a slope of $x = -1$ and at low M a slope of $x = -^2/_3$ was calculated: (a) for an A−S system and (b) for the detailed MMA−F6MA system.

system, calculations were restricted to a limited number of monomeric units. Nevertheless, an estimation of $\tilde{\gamma}_\infty$ could be made, and the corresponding results are given in Figure 7b. It can be seen that the results in Figure 7b show a similar behavior as the simplified homopolymer system. The slope at high molecular weight tends to be slightly smaller than −1. This is most likely due to the inaccuracy in the determination of $\tilde{\gamma}_\infty$.

In summary, we observe that the maximum reduction of surface tension that can be reached with chain length variation (at constant composition) is only of order 10^{-3} in $\tilde{\gamma}$, corresponding to 10^{-4} N/m in γ. This effect is too small to explain the much larger deviations between the experiments and theoretical predictions (Figure 2). We therefore conclude that the polydispersity in chain length is not responsible for the deviation.

D. Chemical Composition Variation. As mentioned before, not only polydispersity in chain length but also polydispersity in chain composition can influence the surface tension. Polydispersity in chain composition implies that some chains contain more fluorinated moieties then others. Consequently, in such a case we are dealing with a polymer blend system, for which can be expected that the surface will be enriched with the component with lower surface tension, i.e., the one with the higher fraction of F6MA.

Surface segregation phenomena have been studied extensively in the past for both miscible and immiscible blends. In these calculations the interest was focused on the determination of the surface excess of one component without considering the change in surface tension of the system. Therefore, we explored the effect of polydispersity in composition on the surface free energy for a blend system of r-$(MMA)_{59}(F6MA)_1$ and r-$(MMA)_{58}(F6MA)_2$ with molar fractions of φ_1 and φ_2, respectively.

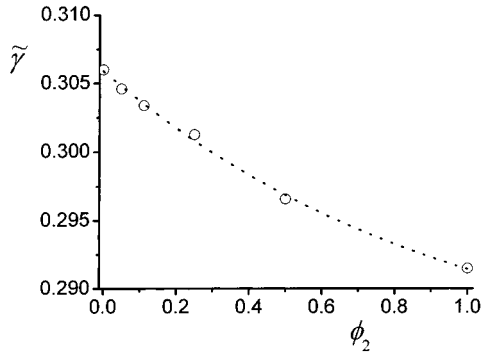

Figure 8. Influence of blend composition on the surface energy as analyzed by the SCF model.

From Figure 8 it can be seen that the surface tension $\tilde{\gamma}$ gradually decreases with increasing amount of MMA_{58}-$F6MA_2$ in the blend (open circles). The points at $\varphi_2 = 0$ and $\varphi_2 = 1$ represent monodisperse systems, but all points at intermediate values of φ_2 represent polymers that are polydisperse in composition. In Figure 2 the dotted line through the SCF results represents the dependence of $\tilde{\gamma}$ for regular polymers, monodisperse in composition. It appears that the dotted line from Figure 8 perfectly overlaps with the dotted line through the monodisperse polymers in Figure 2. This suggests that slight polydispersity in composition for regular copolymers do not lead to drastic reduction in surface tension.

E. Chain Architecture Dependency. As seen in the previous sections, the influence of both polydispersity of molecular weight and chemical composition is not large enough to account for the differences between the SCF analyses and the experimental data in the surface tension at low F6MA content in the polymer. Generally random copolymers are disperse in composition. Moreover, the sequence of monomer units along the chain may not be ideally random; any composition drift along the chain will give the copolymer, to some extent, the character of a block copolymer.

In our SCF analysis so far we only considered regular copolymers. In this section the influence of nonregularity of the distribution of the F6MA monomers along the chain will be investigated, viz. the influence of blockiness. Two parameters of blockiness will be studied: (i) the size of the block and (ii) the position of the block in the polymer chain. The first F6MA unit in the block defines the position in the chain. Thus, in the polymer *b*-$(MMA)_8(F6MA)_5(MMA)_{47}$ the block of 5 F6MA units starts at position 9 of the polymer chain.

A dramatic effect on the surface tension is observed when blockiness is introduced into to polymer chain (Figure 9). Upon changing the chain architecture from *r*-$(MMA)_{55}(F6MA)_5$ to *b*-$(MMA)_{55}(F6MA)_5$ a reduction in $\tilde{\gamma}$ was observed from 0.264 (Figure 2) to 0.151.

When analyzing the effect of blockiness in more detail (Figure 9), we observe that upon changing the block position for each block length, from the end to the middle, a gradual increase in $\tilde{\gamma}$ occurs. Furthermore, it can be seen that increasing the block length will lead to a decrease of the surface tension. The effects of polydispersity in architecture on the surface tension of the polymer melt can therefore well explain the difference between our SCF and experimental data as shown in Figure 2.

We have seen that the surface conformation of the partially fluorinated polymethacrylates is dominated by the large affinity of fluorine toward the liquid−vapor interface. In Figure 10 the density profiles are shown for three different polymer architectures with the same overall composition. It can be seen that three morphology transitions can be observed. A single fluorine enriched layer in the liquid−vapor interface is found for the polymer *r*-$(MMA)_{55}(F6MA)_5$. The enrichment is followed by a depletion zone similar as was observed for *r*-$(MMA)_{57}(F6MA)_3$ in Figure 3. When the five F6MA segments are grouped together in the middle of the polymer chain, an interesting oscillatory density profile is found. These oscillations arise from the preference of the fluorinated moieties for the surface. In this density

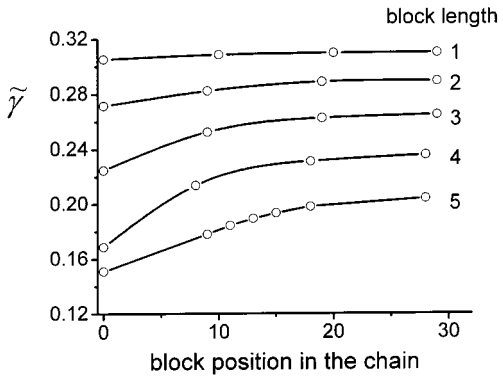

Figure 9. Influence of the size and chain position of blockiness on the surface tension of the polymer melt.

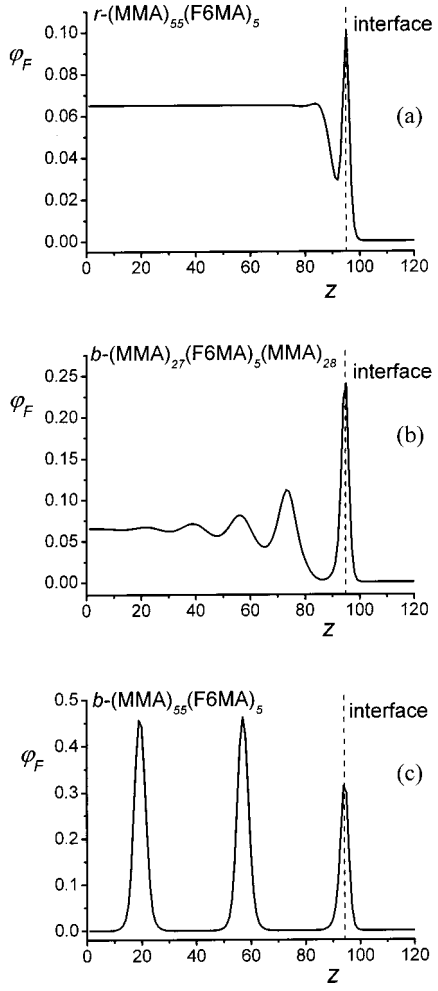

Figure 10. Density profiles of φ_F for the polymers: (a) *r*-$(MMA)_{55}(F6MA)_5$, (b) *b*-$(MMA)_{27}(F6MA)_5(MMA)_{28}$, and (c) *b*-$(MMA)_{55}(F6MA)_5$.

profile the tendency toward surface-induced ordering of a lamellar phase is already very strong. Moreover, the surface ordering suggests that the system is close to a microphase separation transition (MST). This type of density profiles typically occur also in sophisticated (liquid-state) PRISM theories of polymers near a solid wall.[39] In such PRISM analysis, the oscillatory structures are on a smaller length scale than in our case and originate from packing effects.

Microphase separation in the bulk can be observed when the fluorinated block is placed at the end of the polymer chain (Figure 10c). Here a completely ordered bulk with lamellae parallel to the surface is visible.

5. Discussion

The SCF theory predicts a nonlinear dependence of the surface tension of a polymer melt as a function of the degree of fluorination of the chains. When the perfluoroalkyl side chains are regular distributed along the chain, it was found that the theory strongly underestimated this nonlinearity as compared to experimental data. It is noteworthy that for all regular distributed compositions the polymer melt remain homogeneous. A significant change in physical behavior is observed when the fluorinated units were grouped together forming a blocked molecule. This change is seen both in the surface tension as well as in the (surface) structure. Already at a low degree of fluorination (small blocks), the surface tension is significantly reduced as compared to the regular case. On top of this, it was found that the polymer melt does not necessarily remain homogeneous. These two aspects are of interest from both a theoretical and a practical point of view. The effect of blockiness may be used to explain the disparity between the theoretical and experimental data for the surface tension as a function of the amount of perfluoroalkyl side chains in the molecule. In random copolymers it should be expected that some type of blockiness exists, and therefore the surface tension in the experimental systems is possibly strongly affected by the preferential adsorption of chain with a blocky nature. The results also show that there is a nonmonotonic effect on the stability of the melt with respect to microphase segregation on the length of the fluorine block. Both for very small blocks as well as for very long blocks the bulk will remain homogeneous, whereas for intermediate cases an inhomogeneous bulk may be found.

The relative low surface tension found experimentally at relatively low F6MA content could only be recovered in the theoretical analysis for blocky chains. We haste to mention that this does not mean that the theoretical calculations proof that our polymer melt in the experimental system is microphase separated. Again, in the experimental system one should expect various types of polydispersities. Some of the molecules may therefore be very surface active. Above we analyzed chains with a single F6MA block. However, it may well be that other types of polydispersity, such as the occurrence of several small groups of F6MA groups at close proximity along the chain may be present. These chains preferentially accumulate at the melt air interface and reduce the surface tension significantly. At the same time the bulk may remain homogeneous in composition because the remaining chains may have their fluor groups distributed more randomly.

From a practical point of view the results are of interest to translate the phenomena described above into ways of making useful structures in polymer thin films. In this respect the use of surface-driven phase separation seems to be an attractive strategy to make coatings, whose surface properties are different from those of the bulk. The final result will then be a stratified film where the fluorinated species have formed a layer facing the coating−air interface. The design of such self-stratifying coatings offers some principal advantages. The first is the economic advantage of effectively applying two coatings in one operation and minimize the necessary amount of expensive perfluorinated materials to create a fluorinated surface. Second, the intercoat adhesion is supposed to be improved. The ultimate goal is to make an ideal coating that combines the best bulk properties with the optimized surface properties.

6. Conclusions

In this paper a molecular-level self-consistent-field theory was used to analyze physical and thermodynamic properties of partially fluorinated methacrylate chains in the vicinity of the polymer−vapor interface. A general formalism was developed for branched polymer systems within the SCF model of Scheutjens−Fleer and was applied to polymer melt−vapor interfaces. Calculations showed that introduction of the perfluorinated side chain leads to a significant reduction of the surface tension. However, the calculated reduction in the surface tension is less pronounced than that observed experimentally.

A number of polymer parameters were investigated to study their influence on the surface tension. Chain length variations, obeying the empirical LeGrand−Gaines relationship, as well as polydispersity in chemical composition were found to have a small influence on the SCF analyses. However, the influence of chain architecture on surface properties appeared to be substantial. Blocked arrays of F6MA units reduce the surface tension to a large extent. Strong effects of the position of the block (end or middle) and the size of the block could be observed. Introduction of blockiness also plays a significant role in the surface composition of these polymers, leading in extreme cases to microphase separation of the bulk with lamellae parallel to the surface.

From the scaled density profiles of the regular copolymers it was observed that the fluorinated tail was located predominately at the boundary of the interface. For reasons of conformational entropy, the CF_3 segments are preferably present in the interface compared to the CF_2 segments. Furthermore, it was found that the depletion layer thickness was linearly related to the square root of m, showing the Gaussian characteristics of the MMA fragment between two F6MA units.

The SCF analyses for partially fluorinated polymethacrylates can be improved by considering flexibility constraints as a function of the grafting density for comblike polymer chains. Some of these aspects have been described previously showing a preferred enrichment of the "stiffer" chains in blends of polymer melts, which has been explained by entropic effects: the stiffer polymers lose less entropy when adsorbing at the interface than the flexible ones.[40]

Acknowledgment. This research was financially supported by the Foundation for Chemical Sciences,

Priority Program Materials (CW-PPM) in The Netherlands.

References and Notes

(1) For example: (a) Pan, D. H.; Prest, J. W. M. *J. Appl. Phys.* **1985**, *28*, 8621. (b) Bhatia, Q. S.; Pan, D. H.; Koberstein, J. T. *Macromolecules* **1988**, *21*, 2166. (c) Jones, R. A. L.; Norton, L. J.; Kramer, E. J.; Bates, F. S.; Wiltzius, P. *Phys. Rev. Lett.* **1991**, *66*, 1326.

(2) For example: (a) Siow, K. S.; Patterson, D. *J. Chem. Phys.* **1973**, *74*, 356. (b) Ober, R.; Paz, L.; Taupin, C.; Pincus, P.; Boileua, S. *Macromolecules* **1983**, *16*, 50.

(3) For example: (a) Shull, K. R.; Kramer, E. J. *Macromolecules* **1990**, *23*, 4769. (b) Shull, K. R.; Kramer, E. J.; Hadziioannou, G.; Tang, W. *Macromolecules* **1990**, *23*, 4780. (c) Liebler, L. *Macromol. Chem., Macromol. Sym.* **1988**, *16*, 1.

(4) Wu, S. *Polymer Interface and Adhesion*; Marcel Dekker: New York, 1982; Chapter 3.

(5) Krupers, M.; Slangen, P. J.; Möller, M. *Macromolecules* **1998**, *31*, 2552.

(6) Höpken, J.; Möller, M. *Macromolecules* **1992**, *25*, 1461.

(7) Pospiech, D. U.; Jehnichen, D.; Häussler, L.; Voigt, D.; Grundke, K.; Ober, C.; Körner, H.; Wang, J. *Polym. Prepr. (ACS)* **1998**, *39*, 882.

(8) Bouteiller, V.; Garnault, A. M.; Teyssié, D.; Boileau, S.; Möller, M. *Polym. Int.* **1999**, *48*, 765.

(9) Schmidt, D. L.; Coburn, C. E.; DeKoven, B. M.; Potter, G. E.; Meyers, G. F.; Fischer, D. A. *Nature (London)* **1994**, *368*, 39.

(10) Elman, J. F.; Johs, B. D.; Long, T. E.; Koberstein, J. T. *Macromolecules* **1994**, *27*, 5341.

(11) Kassis, C. M.; Steehler, J. K.; Betts, D. E.; Guan, Z.; Romack, T. J.; DeSimone, J. M.; Linton, R. W. *Macromolecules* **1996**, *29*, 3247.

(12) Thomas, R. R.; Anton, D. R.; Graham, W. F.; Darmon, M. J.; Sauer, B. B.; Stika, K. M.; Swartzfager, D. G. *Macromolecules* **1997**, *30*, 2883.

(13) Iyengar, D. R.; Perutz, S. M.; Dai, C.-A.; Ober, C. K.; Kramer, E. J. *Macromolecules* **1996**, *29*, 1229.

(14) Genzer, J.; Sivaniah, E.; Kramer, E. J.; Wang, J.; Körner, H.; Char, K.; Ober, C. K.; DeKoven, B. M.; Bubeck, R. A.; Fischer, D. A.; Sambasivan, S. *Langmuir* **2000**, *16*, 1993.

(15) Van de Grampel, R. D. Surfaces of Fluorinated Polymer Systems. Ph.D. Thesis, Eindhoven University of Technology, 2002.

(16) Lüning, J.; Stöhr, J.; Song, K. Y.; Hawker, C. J.; Iodice, P.; Nguyen, C. V.; Yoon, D. Y. *Macromolecules* **2001**, *34*, 1128 and references therein.

(17) Van der Linden, C. C.; Leermakers, F. A. M.; Fleer, G. J. *Macromolecules* **1996**, *29*, 1000.

(18) Scheutjens, J. M. H. M.; Fleer, G. J. *J. Phys. Chem.* **1979**, *83*, 1619.

(19) Scheutjens, J. M. H. M.; Fleer, G. J. *J. Phys. Chem.* **1980**, *84*, 178.

(20) Binder, K. *Monte Carlo and Molecular Dynamics in Polymer Science*; Oxford University Press: Oxford, 1995.

(21) (a) Edwards, S. F. *Proc. Phys. Soc., London* **1965**, *85*, 613. (b) Dolan, A. K.; Edwards, S. F. *Proc. R. Soc. London, A* **1974**, *337*, 50.

(22) Fleer, G. J.; Scheutjens, J. M. H. M.; Cohen Stuart, M. A.; Cosgrove, T.; Vincent, B. *Polymers at Interfaces*; Elsevier: London, 1993.

(23) Leermakers, F. A. M.; van Male, J.; Skvortsov, A. M. *Macromolecules* **2001**, *34*, 8294.

(24) Leermakers, F. A. M.; Scheutjens, J. M. H. M. *J. Phys. Chem.* **1988**, *89*, 3264.

(25) Theodorou, D. N. *Macromolecules* **1988**, *21*, 1391.

(26) Evers, O. A.; Scheutjens, J. M. H. M.; Fleer, G. J. *Macromolecules* **1990**, *23*, 5221.

(27) Schlangen, L. J. M.; Koopal, L. K.; Lyklema, J. *J. Phys. Chem.* **1996**, *100*, 3607.

(28) It will influence details; however, it will keep the physical interpretation of the phenomena observed and described intact. For example, it is well-known that CF_3 is more surface active than CF_2.

(29) Zisman, W. A. *Contact Angle, Wettability, and Adhesion*; American Chemical Society: Washington, DC, 1964.

(30) Bates, F. S. *Science* **1991**, *251*, 898.

(31) Sauer, B. B.; Dee, G. T. *J. Colloid Interface Sci.* **1994**, *162*, 25.

(32) LeGrand, D. G.; Gaines, G. L., Jr. *J. Colloid Interface Sci.* **1969**, *31*, 162.

(33) Poser, C. I.; Sanchez, I. C. *J. Colloid Interface Sci.* **1979**, *69*, 539.

(34) Cahn, J. W.; Hilliard, J. E. *J. Chem. Phys.* **1958**, *28*, 258.

(35) De Gennes, P. G. *C. R. Acad. Sci. II* **1988**, *307*, 1841.

(36) Theodorou, D. N. *Macromolecules* **1988**, *21*, 1411.

(37) Kumar, S. K.; Jones, R. L. *Adv. Colloid Interface Sci.* **2001**, *94*, 33.

(38) Jalbert, C.; Koberstein, J. T.; Yilgor, I.; Gallagher, P.; Krukonis, V. *Macromolecules* **1993**, *26*, 3069.

(39) Curro, J. G.; Weinhold, J. D.; McCoy, J. D.; Yethiraj, A. *Comput. Theor. Polym. Sci.* **1998**, *8*, 159.

(40) Yethiray, A.; Kumar, S.; Hariharan, A.; Schweizer, K. S. *J. Chem. Phys.* **1994**, *100*, 4691.

MA0121870